

## **A STUDY OF RESERVOIR ESTIMATION FOR A DEEP-SEATED GEOTHERMAL RESERVOIR USING TOUGH2 AND CHEMTOUGH2.**

Tatusya Sato<sup>1</sup>, Kazumi Ohsato<sup>1</sup>, Takahiro Shiga<sup>1</sup>, Masatake Sato<sup>1</sup>  
Stephen P. White<sup>2</sup>, Warwick M. Kissling<sup>2</sup>

<sup>1</sup> Geothermal Energy Research & Development Co., Ltd.

<sup>2</sup> Industrial Research Ltd.

[tatuya@gerd.co.jp](mailto:tatuya@gerd.co.jp)

### **ABSTRACT**

Two methods are used to estimate the parameters of a deep-seated geothermal reservoir assumed to lie beneath the Uenotai geothermal field located in Japan. In the first temperatures and pressures measured in an already developed shallow reservoir are used to constrain model parameters used in modeling the deep reservoir. The second method matches not only the conventional pressure and temperature measurements but also calculates reservoir chemistry and rock alteration and compares these with measured and observed data from the shallow reservoir.

### **INTRODUCTION**

We have developed a method to estimate the capacity of deep-seated geothermal reservoirs (DSGR) lying beneath existing geothermal reservoirs in Japan. This study was a part of the DSGR project of The New Energy and Industrial Technology Development Organization (NEDO).

Before the drilling stage of DSGR development, we do not have enough data to estimate the capacity of a DSGR. Since the cost of a deep well for DSGR exploration will be high, we need to estimate the capacity of the DSGR using existing shallow reservoir information. In this paper we describe a method for estimating the capacity of the DSGR using a simple model. We then apply this method to an existing geothermal area in Japan. Our estimation method consists of two stages.

1. DSGR reservoir parameters are estimated using techniques such as extrapolation of existing shallow reservoir parameters.
2. A simple numerical reservoir model is prepared using the estimated DSGR reservoir parameters. The DSGR capacity is estimated modeling production from the reservoir with TOUGH2.

For the DSGR the major reservoir parameters to be estimated are a) permeability, b) temperature and c) reservoir volume.

In order to evaluate the method we have applied it to an existing geothermal area in Japan. As we did not have deep reservoir information we constructed a numerical model that included both the deep and shallow reservoirs and compared the estimated reservoir parameters obtained by extrapolation with the values for the deep reservoir of the numerical model that gave the best match to measured shallow data. We constructed two numerical reservoir models for this test case.

**Method A** This numerical model of the test field was constructed using a version of TOUGH2 extended to include thermodynamic functions for super-critical conditions (Kissling 1995, Kissling and White 1999). In this case, an existing numerical model was used for the shallow part. Deep reservoir parameters were set by matching the observed temperature and pressure distribution of the shallow reservoir.

**Method B** This numerical model for the test field was constructed using ChemTOUGH (White 1995). We matched temperature, pressure and chemical information of shallow reservoir.

In this paper, we would like to present the results of these numerical models.

### **DEEP GEOTHERMAL RESERVOIR MODEL**

In this study, we assume that the deep reservoir is an up-flow zone that lies under a shallow reservoir (Figure 1). Meteoric water is heated at the heat exchange layer below a deep reservoir. Heated brine rises to the shallow reservoir through the deep reservoir.

The numerical model includes both the shallow reservoir zone and the deep zone. Below the deep reservoir, there is a heat exchange zone. Under the heat exchange zone, there is basement rock that is impermeable and has a high temperature (over 400° C).

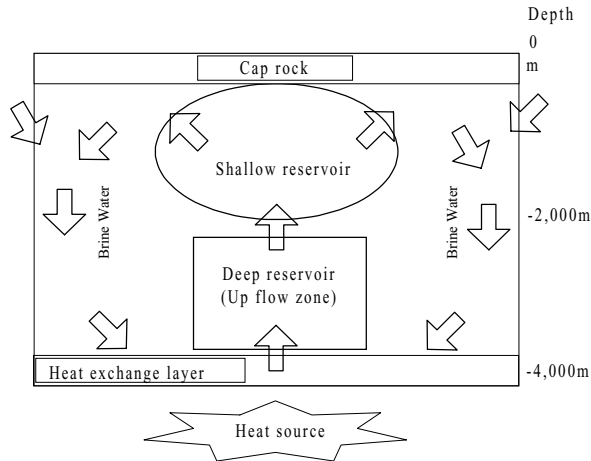


Figure 1. Deep reservoir model

For the shallow reservoir part of the numerical model, we applied an existing numerical model that had been calibrated earlier. If we set reasonable parameters for the deep reservoir, the shallow reservoir will be warmed up and the temperature and pressure distribution will fit with observed values for shallow the reservoir.

This method has been applied to the Uenotai geothermal area and Sumikawa-Onuma geothermal field in Japan (Figure 2). However in this paper we discuss only the Uenotai case.

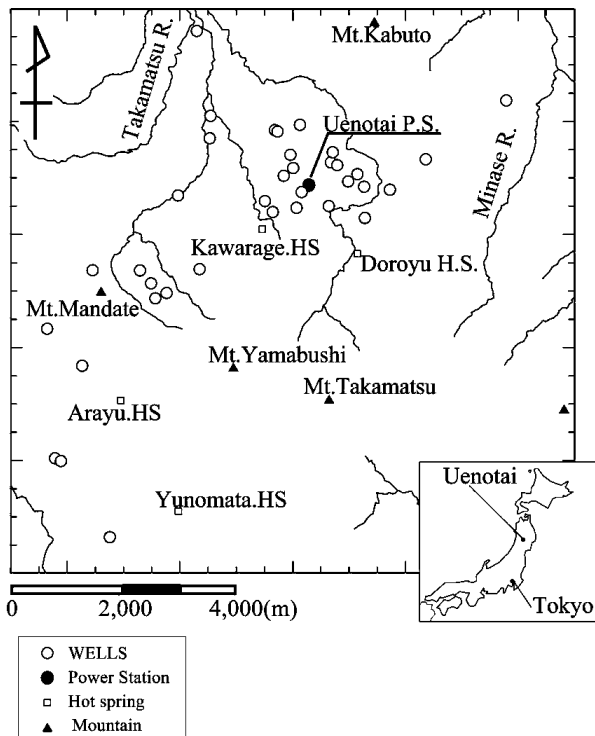


Figure 2. Location of the Uenotai geothermal reservoir.

## NUMERICAL MODELING FOR UENOTAI GEOTHERMAL FIELD.

### Geology of the Uenotai Area

The Uenotai geothermal field is in the Akita prefecture, in the Northern part of Honshu Island, Japan (Figure 2). Gentle domes and basins characterize the geological structure of this area. The Uenotai power plant is located to the North of Mt. Takamatsu and the Onikobe power plant is located to the East of the mountains. These power stations are either on the rim of or the inside basins.

The Ohyu backbone mountains run along the east of the area. The Pre-Tertiary rocks forming the basement underlie the area. Pre-Tertiary rocks consist of greenschist, serpentinite and granodiorite. The Neogene is divided into Doroyu, Minasegawa and Sanzugawa formations. The Quaternary rocks consist of the Kabutoyama formation and the Takamatudake-volcanic rocks. The intrusive rocks consist of Neogene-granite, dacite, andesite and dolerite. The primary faulting runs mainly in a NW-SE direction, NE-SW direction faults are secondary. Geothermal indications such as alteration zones, hot springs and fumarole zones are present along the NW-SE directional fault (Figure 3).

The reservoir within the Uenotai project area is formed primarily by a horst block consisting mainly of Tertiary intrusive rock, pre-Tertiary granitic and metamorphic rocks and lava.

An existing numerical model of this shallow area was used for layers L2-L9. The bottom layer is the heat exchange layer. Brine flows from a side boundary and is heated up. The boundary conditions on the side boundary of the bottom layer are constant temperature and pressure. The lower boundary of the bottom layer is connected to a 420°C heat source (no mass flow). The boundary conditions at the top are 15°C constant temperature and no mass flow.

On layers L5-L6 there is an outflow region on the northwest side. This is modeled as a constant temperature and pressure boundary conditions. Brine from the deep reservoir rises to L5-L6. Layer L7 is low permeability rock and provides a capping structure for the model forcing the flow direction to side boundary that is the outflow zone.

Southwest from Uenotai field, there is the Wasabizawa shallow reservoir (Figure 3). We added the Wasabizawa reservoir in the model. So, this model has two shallow/deep reservoirs.

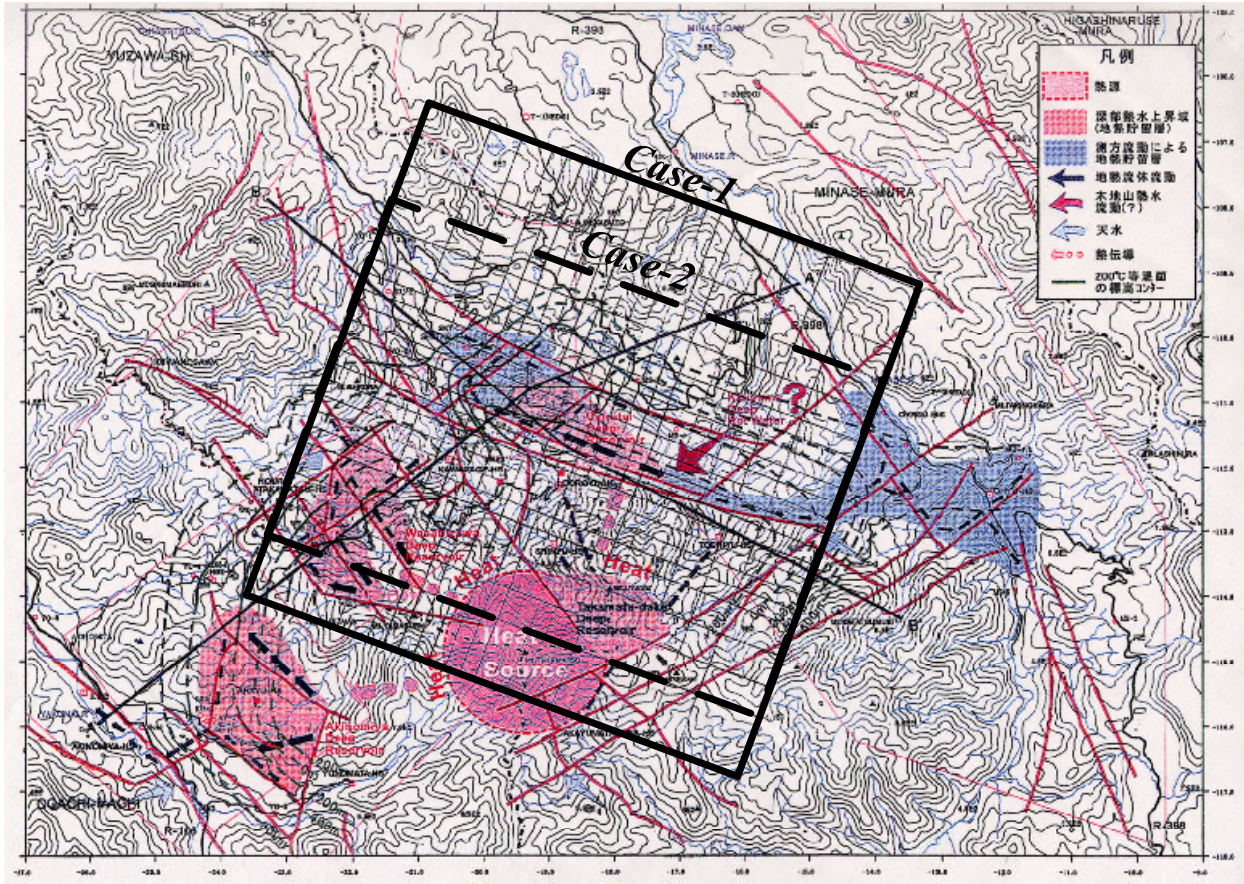


Figure 3. Grid layout for numerical model of the Uenotai geothermal field.

### METHOD A NUMERICAL MODEL

For this work we have used a version of TOUGH2 (Pruess, 1991) that has been modified for super-critical conditions (Kissling, 1999).

The code (EOS11) allows simulations up to 2000°C and 2000 bar. Thermodynamic properties of water are taken from UK Steam Tables (1970) for pressures less than 1000 bar and temperatures below 440°C. Outside this range the equation of state of Haar, Gallagher and Kell (1984) are used. Results from the use of the EOS11 code compare favorably with those in the literature.

For constructing the numerical model, we used GeoCAD (Burnell *et al.* 2003) a preprocessor for TOUGH2. Also we used G-star-base (G\*Base) that is postprocessor/database system for TOUGH2 modeling.

Figure 4 shows the mesh layout of the model and Figure 5 the vertical structure. Layers B2-L1 represent the deep reservoir and layers L2-L9 the shallow.

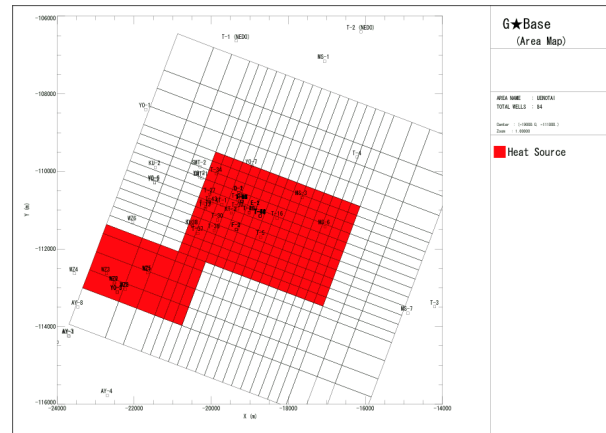


Figure 4. Mesh layout of Case-1.

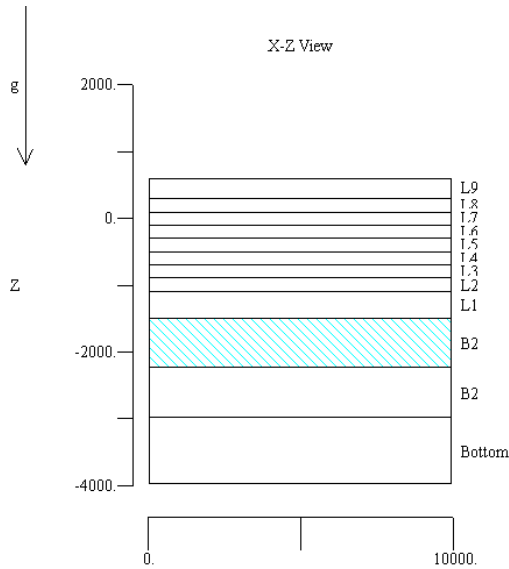


Figure 5. Vertical structure of the model.

**Results of Method A**

In this model, we assume that the deep reservoir is an up-flow zone that lies under the shallow reservoir. If we apply reasonable condition for deep reservoir, the shallow reservoir is warmed and temperature / pressure distribution is fit to the observed data.

For the shallow reservoir we used the parameters from a previously calibrated numerical model. For the deep reservoir, as we had no information because no deep wells had been drilled, we used the lowest permeability and porosity from the shallow reservoir. We expect that permeability and porosity of the deep reservoir will be lower than shallow value.

We tested the sensitivity of the calculated temperatures and pressures in the shallow reservoir to the size of the deep reservoir by running three scenarios. In all cases we assume that the deep reservoir is homogenous.

- Method A (1) Deep reservoir smaller than the shallow reservoir (1.5km<sup>2</sup>)
- Method A (2) Deep reservoir almost same the same size as shallow the reservoir (4.0km<sup>2</sup>)
- Method A (3) Deep reservoir bigger than the shallow reservoir (7.3km<sup>2</sup>).

Figure 7 shows results of this parameter study.

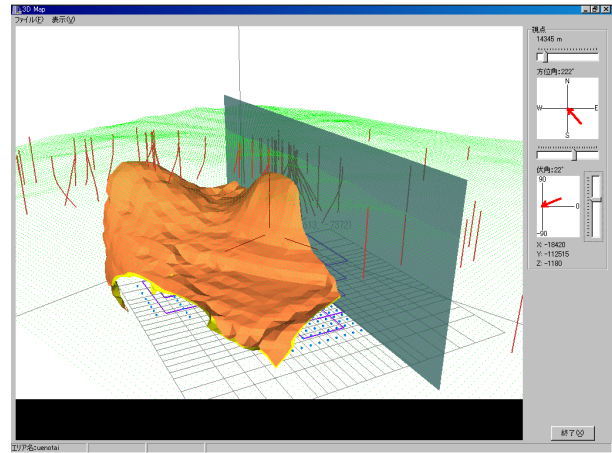


Figure 6. Temperature distribution of Case-1B.

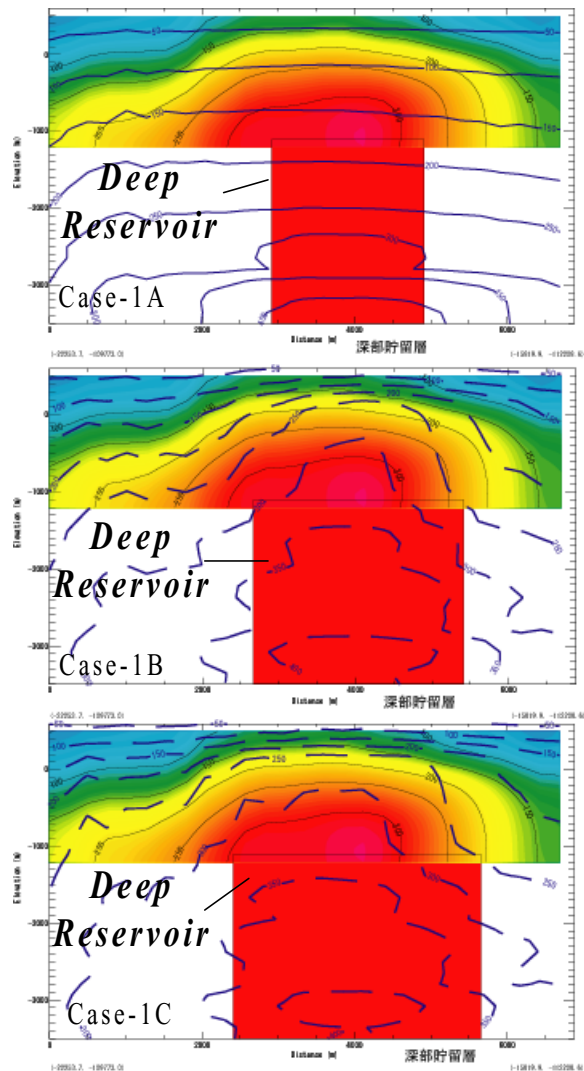


Figure 7. Result of sensitivity study for deep reservoir area.

If the deep reservoir is narrower than the shallow reservoir, temperatures in the shallow reservoir do not reach observed values (Method A(1)). In the other two cases a reasonable match to observed temperatures was obtained.

**MODELLING CHEMISTRY AND ROCK ALTERATION**

**Numerical model**

The grid for Method 2 was a simplified version of the Method 1 model and the horizontal structure is shown in Figure 8. The vertical structure is identical to Method-1 (Figure 5).

Above L2 layer, the permeability structure is identical to the Case-1. Below this layer the reservoir is divided into four different rock types (Figure 9).

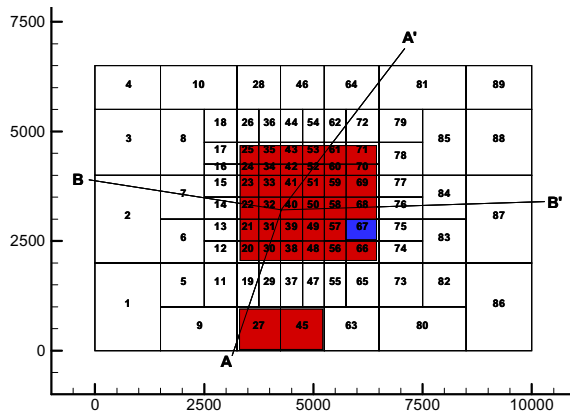


Figure 8. Mesh layout of model and base boundary conditions of Case-2

The permeability of rocks within this low permeability boundary together with heat and mass flows across the bottom of the model are adjusted to provide a good match to the shallow temperatures. The permeabilities for these rocks and heat flows were adjusted using iTOUGH2 to best match the shallow temperatures. There were some problems with this approach. These were not because of problems with iTOUGH2 but rather with the way the supercritical module EOS11 dealt with two-phase sub-critical to super-critical transitions. Considerable effort has been devoted to modeling these transitions correctly and although the problem has not been completely solved we were able to calculate parameters for the deep reservoir that provided a reasonable match to shallow

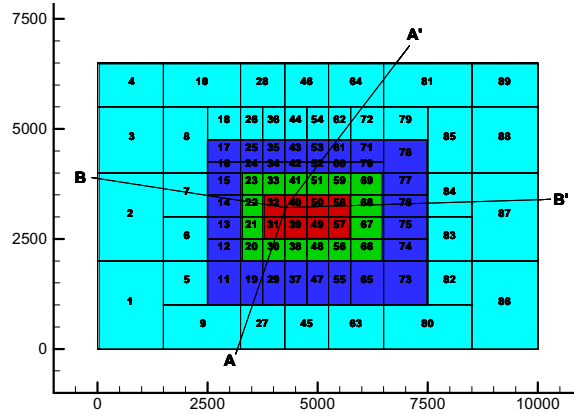


Figure 9. Permeability structure assumed at depth. The innermost region (coloured red) is referred to as D 3, then the surrounding regions as D 2 (green), D 1 (blue) and Outside (cyan).

**Boundary Conditions at the Base**

Several different scenarios were investigated with different boundary conditions at the base of the model; and these are described in the results section. In the base case energy flows into the system at a rate of 13 MW across the bottom boundary. This energy flow is supplied by conduction (11.8 MW) and by a high enthalpy (2000 kJ/kg) source fluid flowing in at a rate of 0.6 kg/s providing a further 1.2MW. This source fluid contains dissolved CO<sub>2</sub>, H<sub>2</sub>S and HCl gases. In terms of the conceptual model proposed by Robertson-Tait *et al.* (1990), it represents diluted type 5 water and forms the parent fluid for the type 2 water found over most of the Uenotai production reservoir.

**High temperature permeability**

Measurements, made in well WD1 (Doi *et al.* 1998) at the Kakkonda field, make it clear that basement rock with a temperature above 380-400° C has very low permeability and the hydrothermal system does not penetrate rocks above this temperature. This effect is ascribed to the rock undergoing an elastic-plastic transition. Once rock has become plastic it will ‘flow’ under a pressure gradient effectively closing the microfractures that provide permeability. White and Mroczek (1998) review the mechanisms for permeability creation and destruction and this paper provides more references on this effect. To take account of this effect we model permeability as reducing linearly over the temperature range 400°C – 420°C. Above 420°C the permeability is set at a fixed value of 10<sup>-3</sup> times the low temperature value.

### **Geology and Geochemistry**

While the general nature of the geology has been investigated and a good description of rock types in the area is available there is little detailed information on the composition of the rocks making up the reservoir. A single composition is assumed for the whole modelled region. We assume the original rock in the reservoir is composed of a mixture of (Na,K,Ca) feldspars and quartz. This is a reasonable approximation to the rock types found in the reservoir and contains the main chemical elements found in the water of the reservoir. Of the measured anions in the reservoir only magnesium and iron are not present in this assumed rock assemblage. The measured amounts of these are very small compared to those included in the modeling.

Modeling the transport of reactive chemicals is a computer intensive activity, and requires that a balance be struck between chemical complexity and calculation time. For the rock assemblage chosen we need to include the reservoir component species,  $H_2O$ ,  $H^+$ ,  $Cl^-$ ,  $SO_4^{2-}$ ,  $HCO_3^-$ ,  $HS^-$ ,  $SiO_2$ ,  $Al^{+++}$ ,  $Ca^{++}$ ,  $K^+$  and  $Na^+$ . These fluid components allow the modelling of reactions between the main magmatic volatiles ( $CO_2$ ,  $H_2S$ ,  $HCl$ ) and the most common rock-forming minerals (albite, anorthite, K-feldspar and quartz).

The set of rock alteration minerals included in the final calculation is Laumontite, Wairakite, Quartz, Calcite, Anhydrite and Albite together with the initial mineral assemblage consisting of Albite, Anorthite, K-Feldspar and Quartz.

### **Thermodynamic data**

The SOLTHERM database (Reed 1992) provides equilibrium constants as a function of temperature for all the reactions considered in this work up to a temperature of 350°C. It appears none of the widely available chemical databases provides data above this temperature explicitly. The program SUPCRT92 (Johnson *et al.* 1992) and associated databases provide a theoretical prediction of equilibrium constants for almost all the reactions of interest at temperatures up to 415° C. There is excellent agreement between theoretical predictions of SUPCRT92 and the SOLTHERM database in regions where they overlap.

It is not possible to calculate the activity coefficients for charged species near the critical point of water. The approach we have taken is to use the values for equilibrium constants and activity coefficients for 350°C for all temperatures greater than 350°C.

### **Modelling Software**

For this work we have used a version of TOUGH2 (Pruess 1991) that has been modified to include the transport of reacting chemicals. The original code was capable modelling temperatures up to 350°C and pressures up to 100 MPa. This has been extended to temperatures up to 800°C but the pressure limit of 100 MPa remains (White and Mroczek 1998).

We have ignored the solubility of all neutral aqueous species in the gas phase even though it may be significant between 360 - 374°C with pressures on the saturation line. Carbon dioxide and hydrogen sulfide gases are included in the simulation as is the effect they have on the saturation pressure of water.

### **Results**

Three scenarios are presented and the parameters for these are given in Table 1. Method-2A assumes poor permeability at depth and energy is transferred to the field primarily by heat conduction. It was necessary to reduce the rate of fluid flow at the base in this scenario otherwise the calculated pressures exceeded the limits of the software (100 MPa). This pressure represents a pressure about 60 MPa in excess of hydrostatic and we believe this is unrealistic. If pressures did reach this level it is expected that permeability would be created through host rock failure and the assumption of low permeability would not be correct.

*Table 1. Permeability and heat and mass flow into the base of the three Case 2 models.*

Parameter	Method 2A	Method 2B	Method 2C
D1 Permeability (m <sup>2</sup> )	1.0×10 <sup>-17</sup>	3.8×10 <sup>-16</sup>	3.8×10 <sup>-16</sup>
D2 Permeability (m <sup>2</sup> )	1.0×10 <sup>-17</sup>	5.8×10 <sup>-14</sup>	1.9×10 <sup>-15</sup>
D3 Permeability (m <sup>2</sup> )	1.0×10 <sup>-17</sup>	3.9×10 <sup>-15</sup>	1.9×10 <sup>-15</sup>
Outside Permeability (m <sup>2</sup> )	1.0×10 <sup>-19</sup>	1.0×10 <sup>-19</sup>	1.0×10 <sup>-19</sup>
Conduction across base	11.8 MW	11.8 MW	12.7 MW
Convection across base	0.3 MW	1.2 MW	1.5 MW

Method-2B had high permeability in the deep reservoir and used the permeabilities calculated using iTOUGH2. Inspection of the temperature distribution calculated for this scenario shows that it is too cool in the area of the Uenotai reservoir although over the full area of the model it gives a reasonable match.

Method-2C is a modified version of Method-2B with permeabilities and heat flow adjusted to improve the match to temperatures in the productive area of the Uenotai reservoir. Figure 10 – Figure 12 shows location of temperature, pH and Laumontite deposition. On this figure, the estimated maximum depth of Laumontite was plotted. Method-2C shows best fit for them (Figure 12).

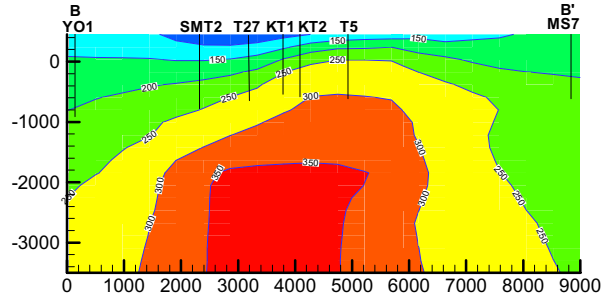


Figure 10. Temperature contours along section B-B' of Case-2C.

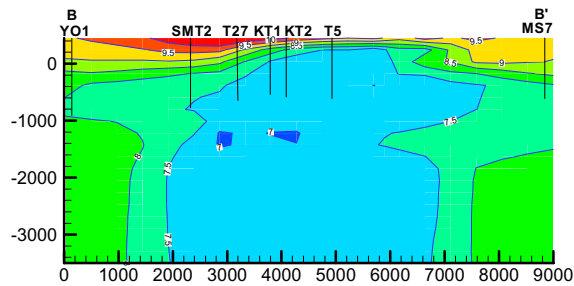


Figure 11. pH contours along section B-B' of Case-2C.

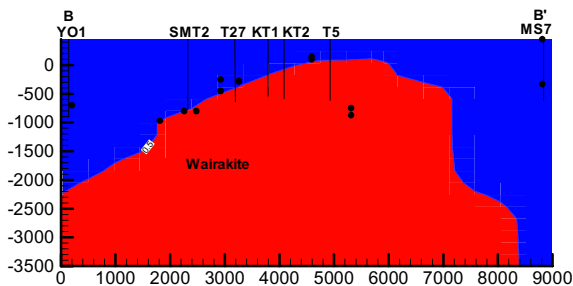


Figure 12. Location of Laumontite (blue) deposition along section B-B' of Case-2C

## CONCLUSION

In this study, we have assumed that the deep reservoir is in an up-flow zone that lies under a shallow reservoir. Meteoric water is heated at the heat exchange layer below the deep reservoir. Heated brine ascends to the shallow reservoir through the deep reservoir.

In this study, we estimated the conditions in the deep reservoir using two methods, one in which only the temperatures and pressures in the shallow reservoir were matched (Method A) and a second in which fluid chemistry and rock alteration in the shallow reservoir were also compared with observation (Method B). We prepared three models for each method. The best model for each method was:

Method A Case B:

- 1) Permeability of deep reservoir  $1.0 \times 10^{-15} \text{ m}^2$  (horizontal),  $1.0 \times 10^{-16} \text{ m}^2$  (vertical)
- 2) Area of deep reservoir  $4.1 - 7.3 \text{ km}^2$
- 3) Average of temperature for deep reservoir  $360^\circ \text{C}$

Method B Case B:

- 1) Permeability of deep reservoir  $1.9 \times 10^{-15} \text{ m}^2$
- 2) Area of deep reservoir  $6.0 \text{ km}^2$
- 3) Average of temperature for deep reservoir  $340^\circ \text{C}$

The results for both cases are similar. We applied these results to develop a simple method to estimate the DSGR capacity. Generally, we are using temperature and pressure data of the natural state to calibrate a numerical mode such as Method-1. Because, we cannot easily use geological information for data fitting.

If we use ChemTOUGH for natural state modeling, it is possible to use the mineral deposit distribution (geological data) for model calibration, although the large amounts of computer time required mean we must use simpler models. Including chemistry and rock alteration increases the amount of data to be matched and helps constrain the model parameters. This should be an advantage for geothermal modeling and we expect that it will produce better models of geothermal fields.

## REFERENCES

Burnell, J.G., White, S.P., Osato, K., Sato, T. GeoCad, a pre and postprocessor for TOUGH2, *Proceedings: TOUGH Symposium 2003*, LBNL, Berkeley, California, May 12–14, 2003

Haar, L, Gallagher, J.S. and Kell, G.S., *NBS/NRC Steam Tables*, Hemisphere Publishing Corp., 320 pp., 1984.

Johnson J.W., Oelkers, E.H., Helgeson, H.C., SUPCRT92: A software Package for Calculating the Standard Molal Thermodynamic Properties of Minerals, Gases, Aqueous Species and Reactions from

1 to 5000 Bar and 0 to 1000° C. *Computers & Geosciences* 18, 7, 1992

Kissling, W.M., Extending Mulkom to super-critical temperatures and pressures. *Proc. World Geothermal Congress* p. 1687, 1995.

Kissling, W.M. and White, S. *Super critical TOUGH2—code description and validation*, IRL internal report 1999.

NEDO, *Report of Deep seated geothermal resource survey* FY1999, 2000.

Pruess, K., TOUGH2—A general purpose numerical simulator for multiphase fluid and heat flow Rep LBL-29400, Lawrence Berkeley Lab., Berkeley, Calif. 1991.

Robertson-Tait, A., Klein, C.W., McNitt, J.R., Naka, T., Takeuchi, R., Iwata, S., Saeki, Y. and Inoue, T. Heat source and fluid migration concepts at the Uenotai geothermal fields, Akita prefecture, Japan. *Geothermal resource Council Transactions*, Vol. 14, Part II, August 1990.

Sato, M. White, S. Osato, K. Sato, T. Okabe, T. Doi, N. Koide, K: Modeling of chemistry and rock alteration at a Deep-seated Geothermal Field, *Proceedings: 25th Stanford Geothermal Workshop*, 2000.

Sato, T., Osato, K., Kissling, W.M., White, S. P., Takahashi, Y., ITO, M., Koide, K., A study of production from a super critical deep seated geothermal reservoir using TOUGH2 numerical simulation, *Proceedings: 21<sup>st</sup> New Zealand Geothermal Workshop*, 2000.

Shiga, T., Sato, S., Sato, T., Okabe, T., Osato, K., Takahashi, Y., Inoue, T., White, S.P., Koide, K., Estimation of deep reservoir temperature distribution using stochastic methods in the Uenotai geothermal field, *Proceedings: 21<sup>st</sup> New Zealand Geothermal Workshop*, 2000.

U.K. Steam Tables in SI Units, Edward Arnold Ltd., London, 161 pp., 1970.

White, S.P. 1995. Multiphase non-isothermal transport of systems of reacting chemicals, *Water Resour. Res.* 31(7), 1761–1772, 1995.

White, S.P., Christenson, B.W., Modelling the alteration halo of a diorite intrusion, *Proceedings: 20<sup>th</sup> New Zealand Geothermal Workshop*, 1998.